Remote sensing evidence for baroclinic tide origin of internal solitary waves in the northeastern South China Sea

Zhongxiang Zhao and Victor Klemas
Graduate College of Marine Studies, University of Delaware, Newark, Delaware, USA

Quanan Zheng
Department of Meteorology, University of Maryland, College Park, Maryland, USA

Xiao-Hai Yan
Graduate College of Marine Studies, University of Delaware, Newark, Delaware, USA

Received 14 November 2003; accepted 19 February 2004; published 16 March 2004.

[1] Evidence for baroclinic tide origin of internal solitary waves (ISWs) in the northeastern South China Sea is presented, based on 116 internal wave packets observed in satellite images from 1995 to 2001. These wave packets can be divided into two types, a single-wave ISW packet containing only one ISW with/without an oscillating tail, and a multiple-wave ISW packet composed of a group of rank-ordered ISWs. All of the 22 single-wave ISW packets occur in the deep water zone. It is suggested that the ISWs, instead of being generated by the lee-wave mechanism, are developed by nonlinear steepening of the baroclinic tides, which are produced by the strong tidal currents flowing over a ridge in Luzon Strait. This suggestion is verified by an ERS-2 SAR image, which records such an evolution process from a baroclinic tide to a single ISW in its spatial domain. *INDEX TERMS:* 0933 Exploration Geophysics: Remote sensing; 3220 Mathematical Geophysics: Nonlinear dynamics; 4544 Oceanography: Physical: Internal and inertial waves; 4572 Oceanography: Physical: Upper ocean processes. **Citation:** Zhao, Z., V. Klemas, Q. Zheng, and X.-H. Yan (2004), Remote sensing evidence for baroclinic tide origin of internal solitary waves in the northeastern South China Sea, *Geophys. Res. Lett.*, *31*, L06302, doi:10.1029/2003GL019077.

1. Introduction

[2] Large amplitude internal solitary waves (ISWs) have been frequently observed in stratified oceans all over the world, especially on continental shelves [*Colosi et al.*, 2001; *Moum et al.*, 2003] and in marginal seas [*Osborne and Burch*, 1980; *Apel et al.*, 1985]. Previous studies demonstrate that they originate from tide-topography interactions over sharply varying topographic features, such as continental shelf breaks and ocean sills [*Lamb*, 1994; *Farmer and Armi*, 1999; *Colosi et al.*, 2001]. The lee-wave generation mechanism was first advanced by *Maxworthy* [1979] and has been confirmed by field measurements in Massachusetts Bay [*Haury et al.*, 1979] and in the Sulu Sea [*Apel et al.*, 1985]. Recently, another generation mechanism suggests that baroclinic tides provide a link between tide-topography interactions and formation of ISWs [*Gerkema and Zimmerman*, 1995]. First, the tide-topography interactions induce baroclinic tides, or internal waves of tidal frequency; then, internal wave packets develop in the troughs of the baroclinic tides. *Holloway et al.* [1997] showed that this transformation occurs over a considerable distance, rather than immediately next to the topographic features. This generation mechanism has been observed on the Australian northwest shelf [*Holloway et al.*, 1997], on the Portuguese shelf [*Sherwin et al.*, 2002], and on the Oregon shelf [*Moum et al.*, 2003].

[3] In the northeastern South China Sea (SCS), ISWs have been observed at a variety of locations from Luzon Strait to the South China shelf. Previous studies have investigated their nonlinear evolution on a shoaling shelf, such as refraction [*Fett and Rabe*, 1977], interaction [*Hsu and Liu*, 2000], diffraction [*Lynett and Liu*, 2002], and polarity conversion [*Orr and Mignerey*, 2003]. The quasi-periodic appearances of these internal wave packets, either in field measurements or in satellite images, reveal that they are of tidal origin [*Ebbesmeyer et al.*, 1991; *Hsu and Liu*, 2000], nevertheless, the specific generation mechanism remains poorly understood. *Hsu and Liu* [2000] suggested that it is similar to lee-wave formation. *Cai et al.* [2002] showed the possibility of the lee-wave generation mechanism in three gaps in Luzon Strait by numerical experiments using a KdV type equation formulated by *Liu et al.* [1998]. Satellite images are useful in improving our understanding of internal wave generation, because they can observe large horizontal two-dimensional internal wave fields [*Osborne and Burch*, 1980; *Apel*, 2003]. By examining the spatial structure of internal wave packets in satellite images, we suggest that the ISWs are developed through nonlinear steepening of baroclinic tides. In this study area, the evolution processes occur in the deep water zone, rather than on the continental shelf as studied by *Holloway et al.* [1997].

2. Satellite Observations and Interpretation

[4] In the northeastern SCS, we have observed 116 internal wave packets in remote sensing images taken by a variety of satellites, such as ERS-1/2, RADARSAT-1 and SPOT, from 1995 to 2001. We compiled a spatial distribution map by placing all these internal wave packets at their corresponding locations (Figure 1). For clarity, each internal wave packet is indicated by its leading ISW. Some internal wave packets are only partly observed, due to limited coverage of the satellite images. The convex curvatures of

0094-8276/04/2003GL019077$05.00

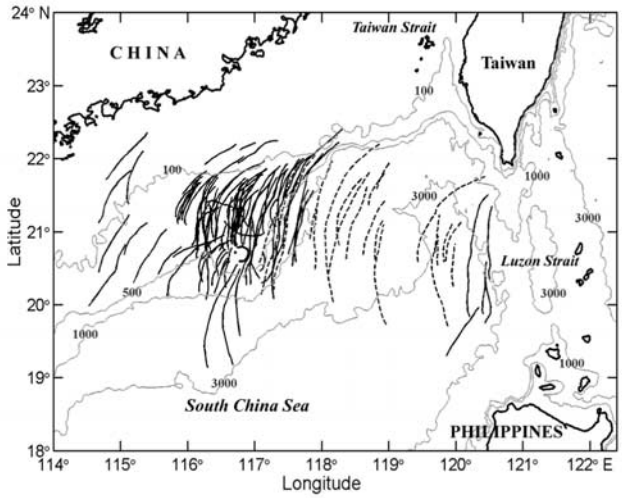

Figure 1. Distribution map of internal wave packets observed in satellite images acquired from 1995 to 2001. Each solid line represents a multiple-wave ISW packet. Each dashed line represents a single-wave ISW packet, which contains an ISW with/without an oscillating tail. The lighter lines indicate isobaths in meters.

the internal wave packets reveal that most of them are propagating northwestwards, with the exception of those reflected by the Dongsha coral reef and several locally generated internal wave packets at the shelf break. In Figure 1, one can see that the internal wave packets are distributed not only on the South China shelf, but also in the deep water zone near Luzon Strait. Therefore, the only candidate for their birthplace is the ocean ridge in Luzon Strait. This distribution map confirms the previous suggestion that internal waves in the northeastern SCS are generated by tidal currents flowing over varying bottom topography in Luzon Strait [*Ebbesmeyer et al.*, 1991; *Liu et al.*, 1998; *Cai et al.*, 2002]. These internal waves propagate onto the shoaling South China shelf after passing through a deep water basin.

[5] In these remote sensing images, we observe two types of internal wave packets, which are indicated in Figure 1 using solid and dashed lines, respectively. A solid line represents one internal wave packet that is composed of a group of rank-ordered ISWs, with the longest wavelength appearing at the front and shortest at the rear (hereinafter multiple-wave ISW packet). A dashed line represents one internal wave packet that contains a single ISW with/without an oscillating tail (hereinafter single-wave ISW packet). To our knowledge, the single-wave ISW packet is rarely reported in other internal wave fields. Figure 2 is an ERS-2 SAR image taken on June 25, 1998, showing a single-wave ISW packet that contains one ISW followed by an oscillating tail. The spatial resolution of the ERS-1/2 SAR image is 25 m. This ISW has a crest length of about 150 km and a width of about 2.5 km. It is no wonder that all the internal wave packets on the South China shelf are in the form of multiple-wave ISW packets, because an ISW usually fissions into a packet of rank-ordered smaller ISWs on a shoaling slope, if the depth changes more rapidly than the ISW's adjustment time scale. In particular, all of the 22 single-wave ISW packets occur in the deep water zone, which reveals that a newborn internal wave packet in the deep water zone is usually a single-wave ISW packet.

[6] For the generation of a multiple-wave ISW packet, *Apel* [2003] suggested that, as time advances, the number of oscillations increases, one per buoyancy period. *Cai et al.* [2002] show that the lee-wave mechanism generates packets of rank-ordered ISWs, alternately propagating westwards and eastwards, over the sills in Luzon Strait. The westward-propagating internal wave packets travel into the SCS. However, the width of the leading ISW in such a packet is about 0.8 km [*Cai et al.*, 2002], much narrower than the single ISW shown in Figure 2. We also find that the single-wave ISW packets appear at least 200 km away from the ridge in Luzon Strait (Figure 1), while internal wave packets generated by the lee-wave mechanism usually appear over the topographic features. Therefore, we do not think that that the single-wave ISW packets are generated by the lee-wave mechanism. It is found that an initial depression could evolve into one or several solitary waves and shed off an oscillating tail, while coming into a balance between nonlinearity and dispersion effects [*Gardner et al.*, 1967; *Dodd et al.*, 1982]. Accordingly, we suggest that the single-wave ISW packets are generated by nonlinear steepening of the baroclinic tides, or large depressions in the stratified oceans.

[7] Fortunately, such an evolution process from a baroclinic tide to a single-wave ISW packet is observed in an ERS-2 SAR image taken on August 3, 2000 (Figure 3). This image covers a sea surface of 100 km × 100 km, centered at 119°50′E, 20°05′N to the west of Luzon Strait. It records only the upper part of an internal wave packet. An intriguing feature is that the brighter stripe width decreases from nearly 5.8 km along section ***A*** to 1.2 km along section ***B*** (Figure 4). Beyond section ***A***, the brighter stripe width becomes much wider, and is barely discernible from the background. In Figure 3, one can see that a darker stripe immediately follows the brighter stripe, although it is not as prominent as the brighter one. In SAR images, an ISW

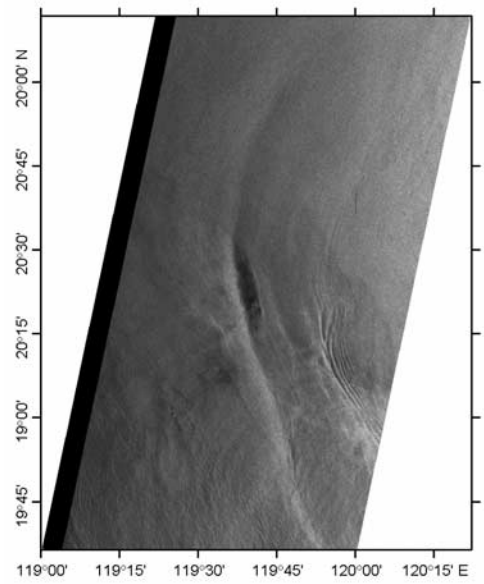

Figure 2. A single-wave ISW packet observed in an ERS-2 SAR image taken on June 25, 1998. Note that it contains only one ISW followed by an oscillating tail.

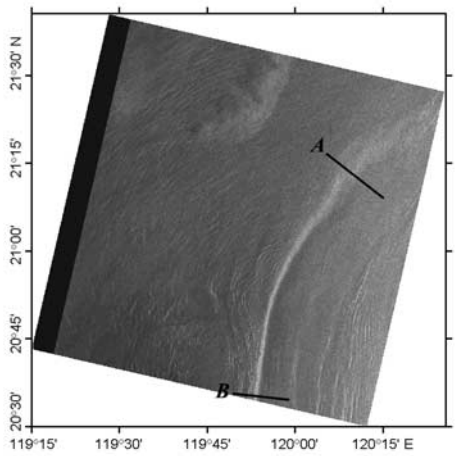

Figure 3. ERS-2 SAR image taken on August 3, 2000 over the deep water zone of the northeastern SCS, showing an ISW of varying width, which is interpreted to be in the middle of an evolution process from a baroclinic tide to an ISW.

usually appears to be a pair of brighter and darker stripes, which correspond to the convergence (rougher) and divergence (smoother) zones, respectively [*Liu et al.*, 1998]. Therefore, we interpret the brighter stripe to be the front face of a depression ISW.

[8] It has been reported that a single satellite image can show different evolution stages of an ISW if the ocean environment is inhomogeneous along the crest direction of the ISW [*Zhao et al.*, 2003]. We suggest the ISW in Figure 3 is in an evolution process from a baroclinic tide to an ISW packet. In this process, the front face of the baroclinic tide becomes steep and narrow. In Figure 3, one can see several ISWs along section ***B***. However, those following behind are not only weaker in image intensity, but also much smaller in wave width than the leading one. Therefore we interpret them to be a single ISW, whose front face is about 1.2 km wide, followed by an oscillating tail, rather than a packet of rank-ordered ISWs [*Zheng et al.*, 2001]. Along section ***A***, it is only an ISW, whose front face is nearly 5.8 km wide. The ISWs along different sections of the crest are in different evolution phases from section ***A*** to section ***B***. Beyond section ***A*** is a baroclinic tide. The wave gradient of a baroclinic tide is much gentler than that of an ISW, so that the convergence zone is wider and almost invisible in SAR images. The spatial inhomogeneity of the ocean environment, for example, variations of background currents, shear, and stratification structure along the crest direction, can cause the lower part of the initial depression develop earlier than the upper part. Another possible reason is that the southern and northern edges of the initial depression are smaller in amplitude, which means they evolve into internal wave packet more slowly. In all, the temporal evolution process from an internal tide to a single-wave ISW packet was recorded in spatial domain of the satellite image. This observation confirms that a single-wave ISW packet in the northeastern SCS is developed through nonlinear steepening of a baroclinic tide.

3. Discussion and Conclusions

[9] On the topography map of the northeastern SCS (Figure 5), one can see that an ocean ridge along 122°E in Luzon Strait separates the SCS and the West Pacific. It was reported that the tidal motion in the SCS is mainly maintained by the energy transported from the West Pacific through Luzon Strait, where the westward tidal energy flux densities of M_2 and K_1 constituents can be as high as 100 kW/m each [*Fang et al.*, 1999]. It is reasonable to assume that the barotropic tidal modes transform into baroclinic tidal modes by the barrier effect of the ridge when passing through Luzon Strait [*Merrifield et al.*, 2001; *Apel*, 2003]. As suggested by *Gardner et al.* [1967], the large amplitude baroclinic tide eventually develops into one ISW by nonlinear steepening, with/without shedding off an oscillating tail, until the nonlinearity and dispersion effects come into balance. Other ocean environment factors, such as rotational effects, horizontal variation of the background currents, shear, stratification, and topography, as well as interactions with other waves and eddies, also play an important role in the evolution process [*Lamb and Yan*, 1996].

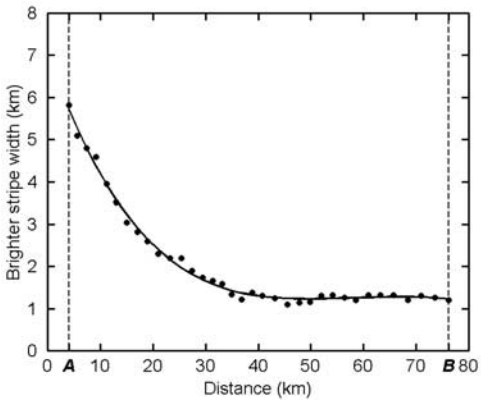

Figure 4. Brighter stripe width of the single ISW shown in Figure 3, revealing the ISW is in a different evolution phase going from section ***A*** to section ***B***.

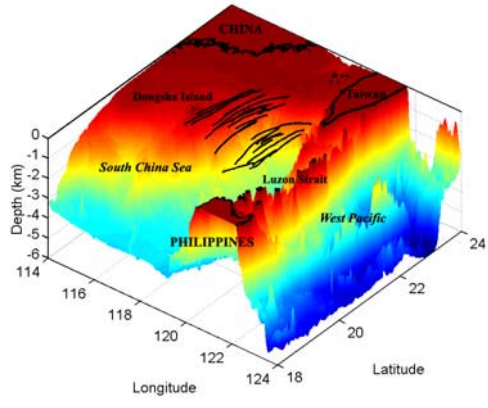

Figure 5. Three-dimensional bottom topography of the northeastern SCS, showing an ocean ridge in Luzon Strait that links the SCS and the West Pacific. The lines indicate internal wave packets in the deep water zone.

[10] The internal wave packets in our case are in the form of single-wave ISW packet. On the northwest Australian shelf, however, *Holloway et al.* [1997] observed that a baroclinic tide steepens and disintegrates into a packet of rank-ordered ISWs (multiple-wave ISW packet) in the trough of the baroclinic tide. As we mentioned above, an ISW can disintegrate into a packet of rank-ordered smaller ISWs while propagating onto a shoaling shelf. In our study area, the nonlinear evolution processes of the baroclinic tides occur in the deep water zone, rather than on a shoaling shelf. Compared with a shoaling shelf, the deep water zone is a favorable condition where a single-wave ISW packet is formed in a depression trough of the baroclinic tides.

[11] In the deep water zone between 120°E and 121°E, we also observe three multiple-wave ISW packets (Figure 1). Their appearances have no relation with seasons, as they occur on June 16, 1995; January 17, 1998; and February 27, 1998; respectively. The widths of the leading ISWs in these three packets are not more than 0.8 km, smaller than the single ISWs observed in the deep water zone. Therefore, we reject the possibility that they are forerunners of the single-wave ISW packets. These multiple-wave ISW packets may be generated by the lee-wave mechanism suggested by *Cai et al.* [2002], or by the nonlinear evolution of baroclinic tides under abnormal ocean conditions, such as a sharp variation in pycnocline along the propagation direction. Whether or not these multiple-wave ISW packets can survive in traveling across the deep water basin is unknown.

[12] In summary, by examining the spatial characteristics of internal wave packets in satellite images, we bring up evidence to demonstrate that the ISWs in the northeastern SCS are generated by nonlinear steepening of baroclinic tides, which are induced by tide-topography interactions in Luzon Strait. An evolution process from a baroclinic tide to an ISW is observed in the spatial domain of an ERS-2 SAR image taken on August 3, 2000. However, details of the nonlinear evolution of a baroclinic tide and the effects of other environment factors, such as the Kuroshio intrusion, still need to be investigated. The statistical results obtained from satellite images in this study can help plan future field measurements of the evolution process.

[13] **Acknowledgments.** This work was partially supported by the ONR Physical Oceanography Program through Grants N00014-97-1-0648 and N00014-03-1-0337. Xiao-Hai Yan is also supported by NASA through Grant NAG5-12745. Images courtesy of Center for Space and Remote Sensing Research, National Central University, Taiwan.

References

Apel, J. R., J. R. Holbrook, A. K. Liu, and J. J. Tsai (1985), The Sulu Sea internal soliton experiment, *J. Phys. Oceanogr.*, *15*, 1625–1651.

Apel, J. R. (2003), A new analytical model for internal solitons in the oceans, *J. Phys. Oceanogr.*, *33*, 2247–2269.

Cai, S., X. Long, and Z. Gan (2002), A numerical study of the generation and propagation of internal solitary waves in the Luzon Strait, *Oceanol. Acta*, *25*, 51–60.

Colosi, J. A., R. C. Beardsley, J. F. Lynch, G. Gawarkiewicz, C.-S. Chiu, and A. Scotti (2001), Observations of nonlinear internal waves on the outer New England continental shelf during the summer shelf break primer study, *J. Geophys. Res.*, *106*(C5), 9587–9601.

Dodd, R. K., J. C. Eilbeck, J. D. Gibbon, and H. C. Morris (1982), *Solitons and nonlinear wave equations*, Academic, pp. 630.

Ebbesmeyer, C. C., C. A. Coomes, and R. C. Hamilton (1991), New observation on internal wave (soliton) in the South China Sea using acoustic Doppler current profiler, 165–175, in *Marine Technology Society Proceedings*, New Orleans.

Fang, G., Y.-K. Kwok, K. Yu, and Y. Zhu (1999), Numerical simulation of principal tidal constituents in the South China Sea, Gulf of Tonkin and Gulf of Thailand, *Contin. Shelf Res.*, *19*, 845–869.

Farmer, D. M., and L. Armi (1999), The generation and trapping of internal solitary waves over topography, *Science*, *283*, 188–190.

Fett, R., and K. Rabe (1977), Satellite observations of internal wave refraction in the South China Sea, *Geophys. Res. Lett.*, *4*, 189–191.

Gardner, C. S., J. M. Green, M. D. Kruskal, and R. M. Miura (1967), Method for solving the Korteweg-de Vries equation, *Phys. Rev. Lett.*, *19*, 1095–1097.

Gerkema, T., and J. T. F. Zimmerman (1995), Generation of nonlinear internal tides and solitary waves, *J. Phys. Oceanogr.*, *25*, 1081–1094.

Haury, L. R., M. G. Briscoe, and M. H. Orr (1979), Tidally generated internal wave packets in Massachusetts Bay, *Nature*, *278*, 312–317.

Holloway, P. E., E. Pelinovsky, T. Talipova, and B. Barnes (1997), A nonlinear model of internal tide transformation on the Australian Northwest shelf, *J. Phys. Oceanogr.*, *27*, 871–896.

Hsu, M.-K., and A. K. Liu (2000), Nonlinear internal waves in the South China Sea, *Can. J. Remote Sens.*, *26*, 72–81.

Lamb, K. G. (1994), Numerical experiments of internal wave generation by strong tidal flow across a finite-amplitude bank edge, *J. Geophys. Res.*, *99*(C1), 843–864.

Lamb, K. G., and L. Yan (1996), The evolution of internal wave undular bores: Comparisons of a fully nonlinear numerical model with weakly nonlinear theory, *J. Phys. Oceanogr.*, *26*, 2712–2734.

Liu, A. K., S. Y. Chang, M.-K. Hsu, and N. K. Liang (1998), Evolution of nonlinear internal waves in East and South China Seas, *J. Geophys. Res.*, *103*(CC4), 7995–8008.

Lynett, P. J., and L.-F. Liu (2002), A two-dimensional, depth-integrated model for internal wave propagation over variable bathymetry, *Wave Motion*, *1071*, 1–20.

Maxworthy, T. (1979), A note on the internal solitary waves produced by tidal flow over a three-dimensional ridge, *J. Geophys. Res.*, *84*, 338–346.

Merrifield, M. A., P. E. Holloway, and T. M. S. Johnston (2001), The generation of internal tides at the Hawaiian Ridge, *Geophys. Res. Lett.*, *28*(4), 559–562.

Moum, J. N., D. M. Farmer, W. D. Smyth, L. Armi, and S. Vagle (2003), Structure and generation of turbulence at interfaces strained by internal solitary waves propagating shoreward over the continental shelf, *J. Phys. Oceanogr.*, *33*, 2093–2112.

Osborne, A. R., and T. Burch (1980), Internal solitons in the Andaman Sea, *Science*, *108*, 451–460.

Orr, M. H., and P. C. Mignerey (2003), Nonlinear internal waves in the South China Sea: Observation of the conversion of depression internal waves to elevation internal waves, *J. Geophys. Res.*, *108*(C3), 3064, doi:10.1029/2001JC001163.

Sherwin, T. J., V. I. Vlasenko, N. Stashchuk, D. R. G. Jeans, and B. Jones (2002), Along-slope generation as an explanation for some unusually large internal tides, *Deep Sea Res. I*, *49*, 1787–1799.

Zhao, Z., V. Klemas, Q. Zheng, and X.-H. Yan (2003), Satellite observation of internal solitary waves converting polarity, *Geophys. Res. Lett.*, *30*(19), 1988, doi:10.1029/2003GL018286.

Zheng, Q., Y. Yuan, V. Klemas, and X.-H. Yan (2001), Theoretical expression for an internal soliton synthetic aperture radar image and determination of the soliton characteristic half width, *J. Geophys. Res.*, *106*(C12), 31,415–31,423.

V. Klemas, X.-H. Yan, and Z. Zhao, Graduate College of Marine Studies, University of Delaware, Newark, DE 19716, USA. (zzhao@udel.edu)

Q. Zheng, Department of Meteorology, University of Maryland, College Park, MD 20742, USA.